JBC Papers in Press. Published on January 31, 2018 as Manuscript M117.818526
The latest version is at http://www.jbc.org/cgi/doi/10.1074/jbc.M117.818526

Stop codon readthrough generates a C-terminally extended variant of the human vitamin D receptor with reduced calcitriol response

Gary Loughran[1,*], Irwin Jungreis[2], Ioanna Tzani[1,♯], Michael Power[1,♮], Ruslan I Dmitriev[1], Ivaylo P Ivanov[1,≠], Manolis Kellis[2], John F Atkins[1,3,*].

From the [1] School of Biochemistry and Cell Biology, University College Cork, Cork, Ireland; [2] CSAIL, Massachusetts Institute of Technology, Cambridge, MA 02139-4307, USA; [3] Dept. of Human Genetics, University of Utah, Salt Lake City, UT 84112-5330, USA.

Running title: *Novel variant of the human vitamin D receptor*

♯Present address: National Institute for Bioprocessing Research and Training, Dublin, Ireland;
♮Present address: Institute for Ophthalmic Research, University of Tübingen, Tübingen, Germany;
≠Present address: Laboratory of Gene Regulation and Development, Eunice Kennedy Shriver National Institute of Child Health and Human Development, National Institutes of Health, Bethesda, Maryland, USA

* To whom correspondence should be addressed. John F. Atkins: Tel: +353 21 4205420; Fax: +353 21 4205462; Email: j.atkins@ucc.ie. Gary Loughran: Tel: +353 21 4205446; Fax: +353 21 4205462; Email: g.loughran@ucc.ie.

Keywords: Vitamin D, calcitriol, VDR, phyloCSF, stop codon, readthrough

ABSTRACT

Although stop codon readthrough is used extensively by viruses to expand their gene expression, verified instances of mammalian readthrough have only recently been uncovered by systems biology and comparative genomics approaches. Previously our analysis of conserved protein coding signatures that extend beyond annotated stop codons predicted stop codon readthrough of several mammalian genes, all of which have been validated experimentally. Four mRNAs display highly efficient stop codon readthrough, and these mRNAs have a UGA stop codon immediately followed by CUAG (UGA_CUAG) that is conserved throughout vertebrates. Extending on the identification of this readthrough motif, we here investigated stop codon readthrough, using tissue culture reporter assays, for all previously untested human genes containing UGA_CUAG. The readthrough efficiency of the annotated stop codon for the sequence encoding vitamin D receptor (VDR) was 6.7%. It was the highest of those tested but all showed notable levels of readthrough. The VDR is a member of the nuclear receptor superfamily of ligand-inducible transcription factors and binds its major ligand, calcitriol, via its C-terminal ligand-binding domain. Readthrough of the annotated *VDR* mRNA results in a 67 amino-acid-long C-terminal extension that generates a VDR proteoform named VDRx. VDRx may form homodimers and heterodimers with VDR but, compared to VDR, VDRx displayed a reduced transcriptional response to calcitriol even in the presence of its partner retinoid X receptor.

INTRODUCTION

Context dependent codon meaning enriches gene expression. Depending on the nature of relevant context features, the efficiency of specification of the alternative meaning can be set at widely different levels or be subject to regulatory influences. The majority of known occurrences of such dynamic redefinition of codon meaning involve UGA and UAG. Since, in the nearly universal genetic code, these codons usually specify translation termination, specification of an alternative meaning generally involves tRNA competition with release factor for their reading in the ribosomal A-site. In what is commonly

Copyright 2018 by The American Society for Biochemistry and Molecular Biology, Inc.

Downloaded from http://www.jbc.org/ by guest on February 27, 2018

termed stop codon readthrough, a near-cognate tRNA performs the decoding with utility deriving from a proportion of the product having a C-terminal extension with an additional function. In these instances, the identity of the amino acid specified by the UGA or UAG is often, but not always, unimportant. However, when the non-universal amino acids, selenocysteine or pyrrolysine are specified, the selected features are these particular amino acids because of their distinctive properties. [Paradoxically in a species where the meaning of UGA, UAA and UAG has, throughout the body of coding sequences, been reassigned to specify amino acids, their meaning is dynamically redefined, in a context-dependent manner, to specify termination (1, 2).]

Stop codon readthrough is well-known in viral decoding, especially of RNA viruses (3). Just as there are select organisms where RNA editing and ribosomal frameshifting are common, cephalopods (4) and *Euplotes* ciliates (5) respectively, so too stop codon readthrough is unusually common in *Drosophila* (6–8) and related insects (9). However, few instances of stop codon readthrough are known in vertebrate gene decoding. Until relatively recently hardly any instances of experimentally verified conserved mammalian readthrough were known (10, 11), although one of the reported occurrences is at least subject to substantial doubt (12, 13). Recent advances in sequencing technologies paved the way for the advent of ribosome profiling which has identified several potential human readthrough candidates (8, 14, 15). Sequencing advances have also propelled comparative genomics which led to the identification of seven mammalian mRNAs whose expression likely involves stop codon readthrough (7, 16, 17). Subsequent experimental analysis confirmed extended in-frame decoding beyond the annotated stop codon (13, 17–21). Two of these mRNAs, *ACP2* and *SACM1L*, have predicted RNA secondary structures immediately 3' of their stop codons and 3' structural elements are well known stimulators of functionally utilized stop codon readthrough (22–24). The four mRNAs with the highest readthrough efficiencies, in the tissue culture cells tested so far, are *OPRL1*, *OPRK1*, *AQP4* and *MAPK10*. Their readthrough efficiencies range from 6-17% and all have UGA stop codons immediately followed by CUAG. For these four genes, this motif is conserved not only in mammals but throughout vertebrates and the importance of the UGA_CUAG motif was confirmed using a systematic mutagenesis approach (17). UGA_CUAG was also subsequently shown to promote readthrough in mRNAs encoding human malate and lactate dehydrogenases (17, 18, 20). Several earlier studies indicated that a cytidine 3′-adjacent to the stop codon influences readthrough in both prokaryotes and eukaryotes (25, 26) but subsequent studies showed that the termination context effect is not limited to a single 3' nucleotide. The 3' motif, CARYYA, can stimulate efficient readthrough, especially in plant viruses (27–29). In yeast, a similar sequence (CARNBA) can stimulate readthrough (30). Very recently, using reporters expressed in mammalian cell-lines, a comprehensive systematic mutagenesis study identified UGA_CUA among the most highly efficient autonomous readthrough signals (31). Indeed, several alphaviruses employ stop codon readthrough on UGA_CUAG including Middelburg, Ross river, Getah and also Chikungunya (24). Readthrough has also been identified on UGA_CUA in Mimivirus and Megavirus which are the best characterized representatives of an expanding new family of giant viruses infecting Acanthamoeba (32).

A search of all human genes for CUAG immediately following a UGA stop codon indicated that there are 23 instances. Four have positive evolutionary coding potential, as measured by PhyloCSF (33) and these are the four candidates we previously confirmed (17). However, functional readthrough cannot be ruled out for those genes with UGA_CUAG and negative PhyloCSF scores. In fact, readthrough of both malate and lactate dehydrogenases (both harboring UGA_CUAG and both having negative PhyloCSF scores) allows translation of a short peroxisome-targeting motif which has been verified experimentally (18, 20). Here, we investigated stop codon readthrough in all previously untested human mRNAs with UGA_CUAG. Consistent with our previous study showing that UGA-CUA alone can support ~1.5% readthrough (17), all candidates

Downloaded from http://www.jbc.org/ by guest on February 27, 2018

tested here displayed levels of readthrough ranging from ~1.3 – 6.7%. The mRNA encoding the vitamin D receptor (VDR) displayed the highest level of readthrough in this study and was selected for further investigation, however, several other mRNAs, including *ATP10D*, *CDH23*, *DDX58*, *SIRPB1* and *TMEM86B* also display highly efficient readthrough (~5.0%).

The VDR is a member of the nuclear receptor superfamily of ligand-inducible transcription factors. While it is expressed in most tissues, it is most abundant in bone, intestine, kidney and the parathyroid gland. Consistent with its role as a transcription factor, it's expression in tissues and tissue culture cells is low (34). Calcitriol (or 1α,25-dihydroxyvitamin D3) is the ligand for the VDR which mediates the actions of the hormone by ligand-inducible heterodimerization with its partner, retinoid X receptor (RXR). Insufficient concentrations of either calcitriol or the VDR impair calcium and phosphate absorption and hypocalcemia develops which can develop into either rickets in children or else osteomalacia in adults. Dietary vitamin D deficiency is the most common cause of rickets and osteomalacia worldwide. Here we identify a C-terminally extended proteoform of the VDR generated by stop codon readthrough and investigate the effect of this extension on VDR function.

RESULTS

Following identification of the UGA_CUAG readthrough motif (17), searches of all human mRNAs for CUAG immediately following a UGA stop codon identified 23 instances (Supp. Table 1). This is a significant depletion of this combination of four nucleotides compared to expectations based on the frequencies of the individual nucleotides in those positions immediately following a UGA stop codon (39 expected, one-sided binomial p-value 0.004). Six of these were previously described and shown by us and others to promote efficient readthrough (13, 17, 18, 20). To experimentally test the remaining 17 potential readthrough candidates, surrounding sequences were cloned in-frame between *Renilla* and firefly luciferase genes. Recently, we described a modification to the classical dual luciferase reporter system (35) that avoids potential distortions, sometimes observed using fused dual reporters, by incorporating 'StopGo' sequences on either side of the polylinker (13). The advantage is that reporter activities and/or stabilities are not influenced by the product/s of the test sequences. HEK293T cells were transfected and lysates assayed by dual luciferase assay. Readthrough efficiencies were determined by comparing relative luciferase activities (firefly/*Renilla*) of test constructs against controls for each construct in which the TGA stop codon is changed to TGG (Trp). All 17 stop codon contexts displayed readthrough efficiencies greater than UGA_C (0.7% readthrough) alone and ranged from 1.3% to 6.7% (Fig. 1).

Because the *VDR* sequence had the highest readthrough level among these 17 genes, we investigated it further. Bioinformatics analysis provided weak evidence that the 67 amino acid C-terminal readthrough extension to VDR may be functional at the amino acid level in the Old World monkey clade (including apes and human), but probably not in other mammals (Fig. 2). The UGA_CUAG motif is conserved in all the Old and New World monkeys examined, suggesting that translation termination of *VDR* mRNA is not efficient in those species. The second stop codon and reading frame are conserved in gorilla, orangutan, rhesus, crab eating macaque, baboon, and green monkey. Since the chimp genome assembly has a gap at this locus, we examined the sequence of the *VDR* mRNA and found that the second stop codon and reading frame are conserved in that species as well. In gibbon, there is a one-base deletion in the 45th codon that disrupts the reading frame. We used PhyloCSF to see if the region between the two stop codons has evolutionary evidence of coding potential in Old World monkeys. The PhyloCSF score of 35.6 for the *VDR* readthrough region alignment in these species is higher than those of same-sized regions 3' of the stop codon of 97.5% of other transcripts, providing further evidence that translation of the sequence is functional in Old World monkeys. The second stop is not conserved in Marmoset, suggesting that the sequence might not be functional in New World monkeys. A 1-base deletion in the 19th codon in the monkey lineage after it split from bushbaby

Downloaded from http://www.jbc.org/ by guest on February 27, 2018

substantially changed the amino acid sequence, and the alignments offer no evidence of functional readthrough in the more distantly related mammals.

Furthermore, inspection of publically available ribosome profiling datasets from experiments in several different human cell-lines and tissues compiled in the GWIPS-viz genome browser (36) reveals ribosome density extending 3' of the annotated *VDR* stop codon which falls off at the next in-frame stop codon – thus providing strong evidence for the existence of *VDR* stop codon readthrough (Supp. Fig. 1A).

The readthrough assays in Fig. 1 suggest that ~7% of the ribosomes translating the *VDR* mRNA decode its UGA stop codon as a sense codon, thus extending VDR at its C-terminus by an additional 67 amino acids to generate VDRx (extended: Supp. Fig. 1B). To test *VDR* readthrough in the context of the full coding sequence we transfected HEK293T cells with constructs encoding an N-terminal HA-tagged wild-type VDR that also included ~200 nt of 3'UTR (HA-VDR-TGA). Control constructs in which the TGA stop codon was changed to either a sense codon (HA-VDR-TGG: readthrough positive control) or to a non-readthrough double stop codon (HA-VDR-TAATAA: readthrough negative control), were also transfected. Anti-HA immunoprecipitates were immunoblotted with a commercially available anti-VDR and a custom antibody raised against the 67 amino acid VDR readthrough peptide (anti-VDRx). In cells transfected with HA-VDR-TGA and HA-VDR-TAATAA, a protein of ~50 kDa, corresponding to HA-tagged canonical VDR was detected by anti-VDR but not by anti-VDRx (Fig. 3A). Both anti-VDR and anti-VDRx also detected a less abundant protein of ~55 kDa in cells expressing HA-VDR-TGA and this protein co-migrates with the major protein detected in cells expressing HA-VDR-TGG (Fig. 3A). Similar results were also observed for VDR constructs tagged with GFP instead of HA (Supp. Fig. 2). Together these immunoprecipitation experiments provide further evidence for the utilization of stop codon readthrough during *VDR* decoding.

The extensions of N-terminal or C-terminal extended proteins sometimes target proteins to subcellular compartments (18, 20, 37, 38). Subcellular targeting prediction software did not reveal known signals within the VDR extension. In addition, live cell imaging of HeLa cells expressing GFP with the 67 amino acid VDR extension fused to its C-terminus displayed a subcellular distribution similar to GFP alone (Supp. Fig. 3). Normally, hormone receptors like the VDR reside in both the cytoplasm and the nucleus (39). To determine whether VDRx is located in the cytoplasm and nucleus we transfected HeLa cells with constructs expressing GFP N-terminal fusions of VDRx (TGA to TGG) and a mutant VDR (TGA to TAATAA) where readthrough is undetectable (Supp. Fig. 2). Live cell imaging in either resting cells or cells stimulated with calcitriol for 10 min. revealed that the subcellular distribution of VDR and VDRx are almost identical (Supp. Fig. 3), with both displaying cytoplasmic and nuclear localization when resting and when stimulated. Furthermore, anti-HA immunoblots of nuclear and cytoplasmic fractions isolated from cells transfected with HA-VDR or HA-VDRx provide further support that, like VDR, VDRx can localize in both the cytoplasm and nucleus (Fig. 3B). Together, these data suggest that the VDR extension does not dramatically alter or target VDRx to a discernible subcellular location.

Next we explored the possibility that VDRx can form homodimers and heterodimers with VDR and RXRα by co-immunoprecipitation experiments from cells co-transfected with epitope-tagged variants of VDRx, VDR and RXRα. GFP-VDRx co-immunoprecipitates with both HA-VDR and HA-VDRx (Fig. 3C). In addition, GFP-VDR also co-immunoprecipitates with both HA-VDR and HA-VDRx. We could not co-immunoprecipitate HA-RXRα with either GFP-VDR or GFP-VDRx - presumably the gentle lysis required for co-immunoprecipitation experiments limits extraction from the nucleus where VDR-RXRα heterodimers are predominantly localized.

The ligand-binding domain of VDR is encoded by amino acids at its extreme C-terminus (40). Since VDRx extends the VDR C-terminus by an additional 67 amino acids, we set out to determine whether VDRx responds to

Downloaded from http://www.jbc.org/ by guest on February 27, 2018

calcitriol similarly to VDR. Firefly luciferase reporter constructs driven by a minimal promoter with tandem VDR elements (VDRE) from the rat osteocalcin gene were co-transfected with each of the HA-tagged VDR constructs described above and then stimulated with 1 nM calcitriol. Control firefly luciferase reporter constructs harboring mutated VDREs were also included. Calcitriol stimulated relative luciferase activities 5-7 fold in cells co-transfected with either HA-VDR-TGA or HA-VDR-TAATAA, whereas cells co-transfected with HA-VDR-TGG (VDRx) did not respond to calcitriol (Fig. 4A: upper panel). This clear inability of VDRx to transactivate in response to calcitriol cannot be accounted for solely by its slightly lower steady state levels (Fig. 4A: lower panel). Whether VDRx is completely unresponsive to calcitriol or just less responsive was examined by transactivation experiments using a range of calcitriol concentrations. Here, almost 100 times more calcitriol is required for HA-VDR-TGG to elicit the same response as either HA-VDR-TGA or HA-VDR-TAATAA indicating that the ability of VDRx to transactivate is much less responsive to calcitriol than for VDR (solid lines in Fig. 4B). However, transactivation by VDRx is still much higher than in mock-transfected (empty vector) cells where only endogenous levels of VDR are expressed, indicating that VDRx retains some capacity to bind calcitriol and must also retain DNA binding capability.

Although we could not detect VDR or VDRx complexed with RXRα by co-immunoprecipitation (Fig. 3C), co-expressing HA-RXRα together with VDR variants resulted in dramatic calcitriol responsive increases in VDRE-reporter transactivation regardless of which VDR variant is overexpressed (dashed lines in Fig. 4B). Although transactivation by VDRx plus RXRα is still reduced compared to VDR with RXRα, it is clear that the VDR C-terminal extension does not completely abrogate heterodimerization with RXRα.

DISCUSSION

In eukaryotes several factors are known to dramatically affect translation termination efficiency and therefore stop codon readthrough. These include the nucleotide sequences surrounding the stop codon (25, 41–46), trans-acting factors (47–49), abundance of near-cognate tRNAs (50–52), abundance and / or modifications of release factors (53–57) and the presence of mRNA secondary structures (22–24, 58–60). In addition, a role for eIF5A in eukaryotic translation termination has been recently reported (61, 62). Interestingly, the amino acid specified is influenced not only by the identity of the stop codon but also local context and tRNA availability which are likely important considerations for potential treatments of disease-causing premature termination codons (51, 52).

Following on from our previous studies which identified a novel stop codon readthrough context in higher eukaryotes (13, 17), we show here that all human genes with this stop codon motif display readthrough. However, while the UGA_CUAG motif alone seems to be sufficient for ~1.3% readthrough, additional local sequences must also be important since the readthrough efficiencies of mRNAs containing this motif ranges from ~1.3% (*GOTIL1* this study) up to ~17% *OPRL1* (13). Given that we tested only 21 nt surrounding the stop codon, the >10-fold difference between the lowest and highest readthrough contexts must reside in this small region – we are currently attempting to identify this additional readthrough stimulator.

How stop codon context and / or nearby RNA secondary structures influence the competition between productive near-cognate tRNA and eukaryotic factor 1 (eRF1) recognition of stop codons is still unknown. Recent cryo-EM structures of eukaryotic ribosomes complexed with eRF1 docked on a stop codon revealed that nucleotide A1825 of 18S rRNA is flipped so that it stacks on the second and third stop codon bases. This formation pulls the 3' base adjacent to the stop codon into the A-site forming a 4 base U-turn where it is stabilized by stacking against G626 of 18S rRNA (63, 64). Stacking with G626 would be more stable for purines which may explain their statistical bias at the +4 position (25) but still doesn't explain why cytidine appears to reduce termination efficiency more than uracil. One possible explanation for how stop codon contexts influence termination could be that mRNA sequence surrounding the stop

Downloaded from http://www.jbc.org/ by guest on February 27, 2018

codon and / or an RNA secondary structure may restrict the formation of the U-turn within the A-site that appears to be necessary for stop codon recognition by eRF1. Perhaps mRNA bases 3' of the stop codon pair with rRNA bases within the mRNA entrance tunnel, as has been considered for some cases of alphavirus programmed ribosomal frameshifting (65).

Of the 17 readthrough candidates tested in this study we observed highest readthrough efficiencies for VDR (~7%) using a novel dual luciferase reporter system (Fig.1). We also confirm VDR readthrough by western blotting with commercially available VDR antibodies as well as a custom antibody raised against the 67 amino acid VDR extension (Fig. 3). Evidence for endogenous VDR readthrough is provided by the analysis of ribosome profiles indicating that ribosome protected fragments map to the VDR transcript immediately 3' of the annotated stop codon but not beyond the next in-frame stop codon (Supp. Fig. 1). Overall we provide strong evidence that some ribosomes read through the stop codon of the VDR coding sequence to generate a C-terminally extended proteoform, VDRx.

Several studies have shown that readthrough can generate dual-targeted proteoforms (18, 20, 37) but here, TargetP analysis of VDR did not reveal subcellular targeting motifs within the readthrough extension. Consistent with this prediction, live cell imaging of fluorescently labeled VDRx indicates that its subcellular localisation is identical to VDR (Supp. Fig. 3) thus suggesting that there are no cryptic targeting motifs within the new VDRx C-terminus. We also used the Predictor of Natural Disordered Regions (66) algorithm to infer ordered and disordered segments in the VDRx extension which were inferred to be largely disordered. No significant homology was found between the VDRx readthrough peptide sequences and structural domains within the InterProScan (67) or NCBI conserved domains databases (68).

Other protein isoforms of the human VDR have been identified previously by others. A common polymorphism that changes the annotated start codon produces a VDR isoform initiated from a 3' AUG codon with a 3 amino acid N-terminal truncation (69) which has been associated with elevated transactivation activity (70, 71). Another VDR isoform with a 50 amino acid N-terminal extension termed VDRB1 is generated by alternative splicing (72, 73). Since the predicted molecular weight of VDRB1 is almost identical to that predicted for VDRx, caution should be exercised when interpreting immunoblots that use antibodies directed against the VDR coding sequence. VDRB1 only differs from VDR by its extended N-terminus which suggests the likely existence of a C-terminal extended proteoform of VDRB1 (VDRB1x) generated by stop codon readthrough.

The function of VDRx is still unclear and requires further investigation. Phylogenetic approaches allow identification of evolutionarily conserved functional readthrough but cannot reveal instances that either emerged recently or, are not under strong evolutionary selection. Although bioinformatic analysis argues against strong evolutionary selection of the VDR extension beyond Old World monkeys, our studies also indicate that the VDR extension does appear to have an overall negative effect on VDR function since VDRx is less able to elicit a transcriptional response to calcitriol. There are several possibilities for why VDRx elicits a reduced response to calcitriol. Given the proximity of the VDR extension to the ligand-binding domain it would not be surprising if this juxtaposition results in impaired binding to calcitriol.. However, other possibilities include either reduced ability to heterodimerize with RXRα or insufficient recognition of VDREs within the promoters of its transcriptional targets. It should be noted that our findings (Fig. 3C) suggest that VDRx can form heterodimers with VDR, which could potentially antagonize VDR action.

It seems likely that the VDR readthrough extension has recently emerged and can improve organism fitness under some, as yet unidentified, physiological condition that appears to be specific for humans and Old World monkeys. Perhaps another ligand for VDR exists in higher primates that has higher affinity to VDRx than VDR. Interestingly, there is some precedent for other recently emerged VDR variations that include three primate-specific exons (5' leader) (74).

Downloaded from http://www.jbc.org/ by guest on February 27, 2018

EXPERIMENTAL PROCEDURES

Plasmids

For the generation of dual luciferase expression constructs, overlapping oligonucleotide pairs (Integrated DNA Technologies: IDT) containing sequence flanking the stop codons (6 nt 5' and 12 nt 3' - see Supp. Table 2) of the predicted readthrough candidates were annealed and ligated with *PspX*I / *Bgl*II digested pSGDluc (13).

The HA-VDR-TGA expression clone was made by PCR amplifying the VDR coding sequence plus 200 nucleotides of 3'UTR from HEK293T cDNA and then cloned *BamH*I / *Xba*I in-frame with the influenza haemagglutinin (HA) tag in pcDNA3-HA (Invitrogen). HA-VDR-TGG and HA-VDR-TAATAA were generated by two-step PCR mutagenesis using HA-VDR-TGA as template. See Supp. Table 2 for PCR primers. RXRα was synthesized by IDT as a G Block and digested with incorporated 5' *Bgl*II and 3' *Xba*I restriction sites then ligated with *BamH*I / *Xba*I digested pcDNA3-HA to generate HA- RXRα. GFP-VDR fusion constructs were made by sub-cloning the VDR-TGA, VDR-TGG and VDR-TAATAA cassettes from the pcDNA3-HA constructs just described into pEGFP-C3 (Clontech).

Wild-type (WT) and mutant (Mu) VDRE-firefly luciferase fusions were generated by restricting WT and Mu G Blocks (IDT)(see Supp. Table 2 for sequences) with *Sac*I / *Bgl*II then ligating with *Sac*I / *Bgl*II restricted pDLuc (75). *Sac*I / *Bgl*II digestion of pDLuc removes the SV40 promoter and *Renilla* luciferase. All constructs were verified by DNA sequencing.

Cell Culture and Transfections

HEK293T cells (ATCC) and HeLa cells (ATCC) were maintained in DMEM supplemented with 10% FBS, 1 mM L-glutamine and antibiotics. HEK293T cells were transfected with Lipofectamine 2000 reagent (Invitrogen), using the 1-day protocol in which suspended cells are added directly to the DNA complexes in half-area 96-well plates. For transfections shown in Fig. 1 the following were added to each well: 25 ng of each plasmid plus 0.2 µl Lipofectamine 2000 in 25 µl Opti-Mem (Gibco). The transfecting DNA complexes in each well were incubated with 4×10^4 cells suspended in 50 µl DMEM + 10% FBS at 37°C in 5% CO_2 for 24 hr.

For transactivation experiments shown in Fig. 4A the following amounts of DNA were added to each well: 20 ng of VDRE-firefly, 5 ng *Renilla* expressing plasmid and 20 ng of either HA-tagged VDR expressing plasmid or empty vector (MOCK). For transactivation experiments shown in Fig. 4B the following amounts of DNA were added to each well: 20 ng of VDRE-firefly, 5 ng *Renilla* expressing plasmid and 10 ng of each HA-tagged VDR plus 10 ng of either HA-RXRα or empty vector. The transfecting DNA complexes in each well were incubated with 4×10^4 cells suspended in 25 µl DMEM + 10% FBS at 37°C in 5% CO_2 for 1 hr before the addition of calcitriol (ENZO) or ethanol control at the indicated final concentrations for a further 24 hr.

Dual Luciferase Assay

Firefly and *Renilla* luciferase activities were determined using the Dual Luciferase Stop & Glo® Reporter Assay System (Promega). Relative light units were measured on a Veritas Microplate Luminometer with two injectors (Turner Biosystems). Transfected cells were lysed in 12.6 µl of 1 × passive lysis buffer (PLB) and light emission was measured following injection of 25 µl of either *Renilla* or firefly luciferase substrate. Readthrough efficiencies (% readthrough) were determined by calculating relative luciferase activities (firefly/*Renilla*) of TGA constructs and dividing by relative luciferase activities from replicate wells of control TGG constructs. The number of biological replicates for each experiment is indicated in each figure legend. Where possible all data points are presented otherwise mean and standard deviations are presented.

Western Analysis

Cells were transfected in 6-well plates using Lipofectamine 2000 reagent, again using the 1-day protocol described above, with 1 µg of each indicated plasmid. The transfecting DNA complexes in each well were incubated with 10^6 HEK293T cells suspended in 3 ml DMEM + 10% FBS and incubated overnight at 37°C in 5% CO_2. Transfected cells were lysed in 100 µl 1 × PLB. Cytoplasmic and nuclear fractions

Downloaded from http://www.jbc.org/ by guest on February 27, 2018

were isolated using the REAP protocol (76). Proteins were resolved by SDS-PAGE and transferred to nitrocellulose membranes (Protran), which were incubated at 4°C overnight with primary antibodies. Immunoreactive bands were detected on membranes after incubation with appropriate fluorescently labeled secondary antibodies using a LI-COR Odyssey® Infrared Imaging Scanner.

Immunoprecipitation

Cells were lyzed in 700 µl PLB and then incubated with 20 µl of protein G Agarose beads plus anti-HA (3 µg) overnight at 4°C with gentle rocking. The beads were washed with ice-cold 1 × PLB buffer and then removed from the beads by boiling for 5 min. in 2 × SDS-PAGE sample buffer for SDS-PAGE and western blotting. For GFP immunoprecipitation, GFP-Trap (Chromtek) was used following the manufacturer's instructions. Briefly, cells were lysed in 100 µl NP40 lysis buffer (10 mM Tris/Cl pH 7.5; 150 mM NaCl; 0.5 mM EDTA; 0.5% NP-40) then 95 µl lysate was diluted to 700 µl in dilution buffer (10 mM Tris/Cl pH 7.5; 150 mM NaCl; 0.5 mM EDTA) before incubation with 20 µl of GFP-Trap beads for 1 hr at 4°C with gentle rocking. The beads were washed with ice-cold dilution buffer and then removed from the beads by boiling for 5 min. in 2 × SDS-PAGE sample buffer for SDS-PAGE and western blotting.

Fluorescence microscopy

Live cell imaging was performed as described before (77) using an inverted Axiovert 200 fluorescence microscope (Zeiss), equipped with 100×/1.4 Plan Apochromat oil-immersion objective (Zeiss), pulsed excitation module (470 nm, 390 nm LEDs), bandpass filters 510-560 nm (EGFP) and 417-477 nm (Hoechst 33342) and gated CCD camera (LaVision, Biotec). Briefly, HeLa cells were seeded onto 8-well chambers pre-coated with a mixture of collagen IV and poly-D-lysine (Ibidi), allowed to attach (24 hr) and forward transfected for 24 hr with plasmids encoding GFP-VDR fusions as indicated. Prior to live imaging, cells were counter-stained with Hoecsht 33342 (1 mM, 30 min). Fluorescence images were collected before (resting) and after stimulation with D3 (10^{-7} M, 10 min, 37 ^{o}C). Images were exported using ImSpector software (LaVision, Biotec) and combined in Adobe Illustrator CS2.

Antibodies

An affinity purified rabbit polyclonal antibody to the 67 amino acid VDR readthrough peptide was prepared by Proteintech to generate anti-VDRx. The following commercially available antibodies were also used. Rabbit anti-VDR (Abcam: ab109234), mouse anti-HA (Covance: Clone 16B12:), mouse anti-β-actin (Sigma A3853), rabbit anti-DNMT3B (Abcam: ab79822) and rabbit anti-EEF2 (CST: 2332).

PhyloCSF and Bioinformatics Analysis

Human transcript models were obtained from GENCODE version 16 (78). All protein-coding transcripts were searched for the UGA_CUAG readthrough motif at the end of the annotated coding sequence. PhyloCSF was run using the 29mammals parameters on the region between the annotated stop codon and the next in-frame stop codon, not including either stop codon, using the 29 placental mammals subset of the 46-vertebrate hg19 whole-genome MULTIZ alignments (79), which were obtained from the UCSC genome browser (80). To compute the evolutionary coding potential of the VDR readthrough region in Old World monkeys, we computed PhyloCSF using the 58mammals parameters on the subset of the 100-vertebrates hg19 alignments consisting of the species Human, Gorilla, Orangutan, Gibbon, Rhesus, Crab_eating_macaque, Baboon, and Green_monkey. To estimate the significance of this score, we similarly computed PhyloCSF scores of the 66 codons 3' of each unique annotated stop codon. For the sequence of the Chimp VDR mRNA we used NCBI Reference Sequence XM_016923548.1 obtained from https://www.ncbi.nlm.nih.gov/nucleotide/1034096372. Alignments were examined using CodAlignView (Jungreis I, Lin M, Chan C, Kellis M. 2016. CodAlignView. CodAlignView: The Codon Alignment Viewer [Internet]. Available from http://data.broadinstitute.org/compbio1/cav.php).

Downloaded from http://www.jbc.org/ by guest on February 27, 2018

ACKNOWLEDGEMENTS
This work was supported by grants from Science Foundation Ireland (12/IP/1492 and 13/1A/1853 to J.F.A. and 13/SIRG/2144 to R.I.D.). I.J. was supported by National Institutes of Health R01 HG004037 and GENCODE Wellcome Trust grant U41 HG007234. I.T. was supported by an award from the Health Research Board (PhD/2007/04). We are grateful for assistance from Dr. John Mackrill and Michelle Heffernan.

CONFLICT OF INTEREST
The authors declare that they have no conflicts of interest with the contents of this article.

AUTHOR CONTRIBUTIONS
G.L. and J.F.A. conceived and coordinated the study and wrote the paper. G.L. designed, performed and analyzed the experiments shown in Figures 1, 3, 4 and Supplementary Figures 1 and 2. I.J., I.P.I. and M.K. performed motif searches and bioinformatic analysis shown in Figure 2. I.T. generated the HA-VDR constructs and M.P. provided technical assistance. R.I.D. performed and analyzed the experiments shown in Supplementary Figure 3. All authors reviewed the results and approved the final version of the manuscript.

REFERENCES
1. Swart,E.C., Serra,V., Petroni,G. and Nowacki,M. (2016) Genetic Codes with No Dedicated Stop Codon: Context-Dependent Translation Termination. *Cell*, **166**, 691–702.
2. Heaphy,S.M., Mariotti,M., Gladyshev,V.N., Atkins,J.F. and Baranov,P. V. (2016) Novel Ciliate Genetic Code Variants Including the Reassignment of All Three Stop Codons to Sense Codons in *Condylostoma magnum*. *Mol. Biol. Evol.*, **33**, 2885–2889.
3. Firth,A.E. and Brierley,I. (2012) Non-canonical translation in RNA viruses. *J. Gen. Virol.*, **93**, 1385–409.
4. Liscovitch-Brauer,N., Alon,S., Porath,H.T., Elstein,B., Unger,R., Ziv,T., Admon,A., Levanon,E.Y., Rosenthal,J.J.C. and Eisenberg,E. (2017) Trade-off between Transcriptome Plasticity and Genome Evolution in Cephalopods. *Cell*, **169**, 191–202.e11.
5. Lobanov,A. V, Heaphy,S.M., Turanov,A.A., Gerashchenko,M. V, Pucciarelli,S., Devaraj,R.R., Xie,F., Petyuk,V.A., Smith,R.D., Klobutcher,L.A., *et al.* (2016) Position-dependent termination and widespread obligatory frameshifting in Euplotes translation. *Nat. Struct. Mol. Biol.*, **24**, 61–68.
6. Lin,M.F., Carlson,J.W., Crosby,M.A., Matthews,B.B., Yu,C., Park,S., Wan,K.H., Schroeder,A.J., Gramates,L.S., St Pierre,S.E., *et al.* (2007) Revisiting the protein-coding gene catalog of Drosophila melanogaster using 12 fly genomes. *Genome Res.*, **17**, 1823–36.
7. Jungreis,I., Lin,M.F., Spokony,R., Chan,C.S., Negre,N., Victorsen,A., White,K.P. and Kellis,M. (2011) Evidence of abundant stop codon readthrough in Drosophila and other metazoa. *Genome Res.*, **21**, 2096–2113.
8. Dunn,J.G., Foo,C.K., Belletier,N.G., Gavis,E.R. and Weissman,J.S. (2013) Ribosome profiling reveals pervasive and regulated stop codon readthrough in *Drosophila melanogaster*. *Elife*, **2**.
9. Jungreis,I., Chan,C.S., Waterhouse,R.M., Fields,G., Lin,M.F. and Kellis,M. (2016) Evolutionary Dynamics of Abundant Stop Codon Readthrough. *Mol. Biol. Evol.*, **33**, 3108–3132.
10. Yamaguchi,Y., Hayashi,A., Campagnoni,C.W., Kimura,A., Inuzuka,T. and Baba,H. (2012) L-MPZ, a novel isoform of myelin P0, is produced by stop codon readthrough. *J. Biol. Chem.*, **287**, 17765–76.
11. Eswarappa,S.M., Potdar,A.A., Koch,W.J., Fan,Y., Vasu,K., Lindner,D., Willard,B., Graham,L.M., Dicorleto,P.E. and Fox,P.L. (2014) Programmed translational readthrough generates antiangiogenic VEGF-Ax. *Cell*, **157**, 1605–1618.
12. Xin,H., Zhong,C., Nudleman,E. and Ferrara,N. (2016) Evidence for Pro-angiogenic Functions of VEGF-Ax. *Cell*, **167**, 275–284.e6.
13. Loughran,G., Howard,M.T., Firth,A.E. and Atkins,J.F. (2017) Avoidance of reporter assay distortions from fused dual reporters. *RNA*, 10.1261/rna.061051.117.

Downloaded from http://www.jbc.org/ by guest on February 27, 2018

14. Andreev,D.E., O'Connor,P.B., Zhdanov,A. V, Dmitriev,R.I., Shatsky,I.N., Papkovsky,D.B. and Baranov,P. V (2015) Oxygen and glucose deprivation induces widespread alterations in mRNA translation within 20 minutes. *Genome Biol.*, **16**, 90.
15. Yordanova,M.M., Loughran,G., Zhdanov,A. V., Mariotti,M., Kiniry,S.J., O'Connor,P.B.F., Andreev,D.E., Tzani,I., Saffert,P., Michel,A.M., *et al.* (2018) AMD1 mRNA employs ribosome stalling as a mechanism for molecular memory formation. *Nature*, 10.1038/nature25174.
16. Lindblad-Toh,K., Garber,M., Zuk,O., Lin,M.F., Parker,B.J., Washietl,S., Kheradpour,P., Ernst,J., Jordan,G., Mauceli,E., *et al.* (2011) A high-resolution map of human evolutionary constraint using 29 mammals. *Nature*, **478**, 476–482.
17. Loughran,G., Chou,M.-Y., Ivanov,I.P., Jungreis,I., Kellis,M., Kiran,A.M., Baranov,P. V. and Atkins,J.F. (2014) Evidence of efficient stop codon readthrough in four mammalian genes. *Nucleic Acids Res.*, **42**, 8928–8938.
18. Stiebler,A.C., Freitag,J., Schink,K.O., Stehlik,T., Tillmann,B.A.M., Ast,J. and B??lker,M. (2014) Ribosomal Readthrough at a Short UGA Stop Codon Context Triggers Dual Localization of Metabolic Enzymes in Fungi and Animals. *PLoS Genet.*, **10**, e1004685.
19. Chan,C.S., Jungreis,I. and Kellis,M. (2013) Heterologous Stop Codon Readthrough of Metazoan Readthrough Candidates in Yeast. *PLoS One*, **8**, e59450.
20. Schueren,F., Lingner,T., George,R., Hofhuis,J., Dickel,C., G??rtner,J. and Thoms,S. (2014) Peroxisomal lactate dehydrogenase is generated by translational readthrough in mammals. *Elife*, **3**, e03640.
21. De Bellis,M., Pisani,F., Mola,M.G., Rosito,S., Simone,L., Buccoliero,C., Trojano,M., Nicchia,G.P., Svelto,M. and Frigeri,A. (2017) Translational readthrough generates new astrocyte AQP4 isoforms that modulate supramolecular clustering, glial endfeet localization, and water transport. *Glia*, 10.1002/glia.23126.
22. Wills,N.M., Gesteland,R.F. and Atkins,J.F. (1994) Pseudoknot-dependent read-through of retroviral gag termination codons: importance of sequences in the spacer and loop 2. *EMBO J.*, **13**, 4137–44.
23. Houck-Loomis,B., Durney,M.A., Salguero,C., Shankar,N., Nagle,J.M., Goff,S.P. and D'Souza,V.M. (2011) An equilibrium-dependent retroviral mRNA switch regulates translational recoding. *Nature*, **480**, 561–4.
24. Firth,A.E., Wills,N.M., Gesteland,R.F. and Atkins,J.F. (2011) Stimulation of stop codon readthrough: frequent presence of an extended 3' RNA structural element. *Nucleic Acids Res.*, **39**, 6679–91.
25. Brown,C.M., Stockwell,P.A., Trotman,C.N. and Tate,W.P. (1990) Sequence analysis suggests that tetra-nucleotides signal the termination of protein synthesis in eukaryotes. *Nucleic Acids Res.*, **18**, 6339–45.
26. Brown,C.M., Stockwell,P.A., Trotman,C.N. and Tate,W.P. (1990) The signal for the termination of protein synthesis in procaryotes. *Nucleic Acids Res.*, **18**, 2079–86.
27. Skuzeski,J.M., Nichols,L.M., Gesteland,R.F. and Atkins,J.F. (1991) The signal for a leaky UAG stop codon in several plant viruses includes the two downstream codons. *J. Mol. Biol.*, **218**, 365–73.
28. Beier,H. and Grimm,M. (2001) Misreading of termination codons in eukaryotes by natural nonsense suppressor tRNAs. *Nucleic Acids Res.*, **29**, 4767–82.
29. Harrell,L., Melcher,U. and Atkins,J.F. (2002) Predominance of six different hexanucleotide recoding signals 3' of read-through stop codons. *Nucleic Acids Res.*, **30**, 2011–7.
30. Namy,O., Hatin,I. and Rousset,J.P. (2001) Impact of the six nucleotides downstream of the stop codon on translation termination. *EMBO Rep.*, **2**, 787–93.
31. Cridge,A.G., Crowe-Mcauliffe,C., Mathew,S.F. and Tate,W.P. (2018) Eukaryotic translational termination efficiency is influenced by the 3 nucleotides within the ribosomal mRNA channel. *Nucleic Acids Res.*
32. Jeudy,S., Abergel,C., Claverie,J.-M., Legendre,M. and Chenivesse,S. (2012) Translation in Giant Viruses: A Unique Mixture of Bacterial and Eukaryotic Termination Schemes. *PLoS Genet.*, **8**, e1003122.
33. Lin,M.F., Jungreis,I. and Kellis,M. (2011) PhyloCSF: a comparative genomics method to distinguish

Downloaded from http://www.jbc.org/ by guest on February 27, 2018

protein coding and non-coding regions. *Bioinformatics*, **27**, i275–i282.
34. Pike,J.W. and Haussler,M.R. (1979) Purification of chicken intestinal receptor for 1,25-dihydroxyvitamin D. *Proc. Natl. Acad. Sci. U. S. A.*, **76**, 5485–9.
35. Grentzmann,G., Ingram,J.A., Kelly,P.J., Gesteland,R.F. and Atkins,J.F. (1998) A dual-luciferase reporter system for studying recoding signals. *RNA*, **4**, 479–486.
36. Michel,A.M., Fox,G., M. Kiran,A., De Bo,C., O'Connor,P.B.F., Heaphy,S.M., Mullan,J.P.A., Donohue,C.A., Higgins,D.G. and Baranov,P. V. (2014) GWIPS-viz: Development of a ribo-seq genome browser. *Nucleic Acids Res.*, **42**.
37. Freitag,J., Ast,J. and Bölker,M. (2012) Cryptic peroxisomal targeting via alternative splicing and stop codon read-through in fungi. *Nature*, **485**, 522–525.
38. Coldwell,M.J., Hashemzadeh-Bonehi,L., Hinton,T.M., Morley,S.J. and Pain,V.M. (2004) Expression of fragments of translation initiation factor eIF4GI reveals a nuclear localisation signal within the N-terminal apoptotic cleavage fragment N-FAG. *J. Cell Sci.*, **117**, 2545–55.
39. Prüfer,K. and Barsony,J. (2009) Retinoid X Receptor Dominates the Nuclear Import and Export of the Unliganded Vitamin D Receptor. *http://dx.doi.org/10.1210/me.2001-0345*, 10.1210/ME.2001-0345.
40. Rochel,N., Wurtz,J.M., Mitschler,A., Klaholz,B. and Moras,D. (2000) The crystal structure of the nuclear receptor for vitamin D bound to its natural ligand. *Mol. Cell*, **5**, 173–9.
41. Bossi,L. and Roth,J.R. (1980) The influence of codon context on genetic code translation. *Nature*, **286**, 123–7.
42. Cavener,D.R. and Ray,S.C. (1991) Eukaryotic start and stop translation sites. *Nucleic Acids Res.*, **19**, 3185–92.
43. Poole,E.S., Brown,C.M. and Tate,W.P. (1995) The identity of the base following the stop codon determines the efficiency of in vivo translational termination in Escherichia coli. *EMBO J.*, **14**, 151–8.
44. McCaughan,K.K., Brown,C.M., Dalphin,M.E., Berry,M.J. and Tate,W.P. (1995) Translational termination efficiency in mammals is influenced by the base following the stop codon. *Proc. Natl. Acad. Sci. U. S. A.*, **92**, 5431–5.
45. Bonetti,B., Fu,L., Moon,J. and Bedwell,D.M. (1995) The Efficiency of Translation Termination is Determined by a Synergistic Interplay Between Upstream and Downstream Sequences inSaccharomyces cerevisiae. *J. Mol. Biol.*, **251**, 334–345.
46. Cridge,A.G., Major,L.L., Mahagaonkar,A.A., Poole,E.S., Isaksson,L.A. and Tate,W.P. (2006) Comparison of characteristics and function of translation termination signals between and within prokaryotic and eukaryotic organisms. *Nucleic Acids Res.*, **34**, 1959–1973.
47. von der Haar,T. and Tuite,M.F. (2007) Regulated translational bypass of stop codons in yeast. *Trends Microbiol.*, **15**, 78–86.
48. Beznoskova,P., Wagner,S., Jansen,M.E., von der Haar,T. and Vala ek,L.S. (2015) Translation initiation factor eIF3 promotes programmed stop codon readthrough. *Nucleic Acids Res.*, **43**, 5099–5111.
49. Urakov,V.N., Mitkevich,O. V., Safenkova,I. V. and Ter-Avanesyan,M.D. (2017) Ribosome-bound Pub1 modulates stop codon decoding during translation termination in yeast. *FEBS J.*, **284**, 1914–1930.
50. Blanchet,S., Cornu,D., Argentini,M. and Namy,O. (2014) New insights into the incorporation of natural suppressor tRNAs at stop codons in Saccharomyces cerevisiae. *Nucleic Acids Res.*, **42**, 10061–10072.
51. Roy,B., Leszyk,J.D., Mangus,D.A. and Jacobson,A. (2015) Nonsense suppression by near-cognate tRNAs employs alternative base pairing at codon positions 1 and 3. *Proc. Natl. Acad. Sci.*, **112**, 3038–3043.
52. Beznosková,P., Gunišová,S. and Valášek,L.S. (2016) Rules of UGA-N decoding by near-cognate tRNAs and analysis of readthrough on short uORFs in yeast. *RNA*, **22**, 456–66.
53. Kobayashi,Y., Zhuang,J., Peltz,S. and Dougherty,J. (2010) Identification of a Cellular Factor That Modulates HIV-1 Programmed Ribosomal Frameshifting. *J. Biol. Chem.*, **285**, 19776–19784.

Downloaded from http://www.jbc.org/ by guest on February 27, 2018

54. Betney,R., de Silva,E., Krishnan,J. and Stansfield,I. (2010) Autoregulatory systems controlling translation factor expression: Thermostat-like control of translational accuracy. *RNA*, **16**, 655–663.
55. Loenarz,C., Sekirnik,R., Thalhammer,A., Ge,W., Spivakovsky,E., Mackeen,M.M., McDonough,M.A., Cockman,M.E., Kessler,B.M., Ratcliffe,P.J., *et al.* (2014) Hydroxylation of the eukaryotic ribosomal decoding center affects translational accuracy. *Proc. Natl. Acad. Sci.*, **111**, 4019–4024.
56. Feng,T., Yamamoto,A., Wilkins,S.E., Sokolova,E., Yates,L.A., Münzel,M., Singh,P., Hopkinson,R.J., Fischer,R., Cockman,M.E., *et al.* (2014) Optimal Translational Termination Requires C4 Lysyl Hydroxylation of eRF1. *Mol. Cell*, **53**, 645–654.
57. Nyikó,T., Auber,A., Szabadkai,L., Benkovics,A., Auth,M., Mérai,Z., Kerényi,Z., Dinnyés,A., Nagy,F. and Silhavy,D. (2017) Expression of the eRF1 translation termination factor is controlled by an autoregulatory circuit involving readthrough and nonsense-mediated decay in plants. *Nucleic Acids Res.*, **45**, gkw1303.
58. Wills,N.M., Gesteland,R.F. and Atkins,J.F. (1991) Evidence that a downstream pseudoknot is required for translational read-through of the Moloney murine leukemia virus gag stop codon. *Proc. Natl. Acad. Sci. U. S. A.*, **88**, 6991–5.
59. Brown,C.M., Dinesh-Kumar,S.P. and Miller,W.A. (1996) Local and distant sequences are required for efficient readthrough of the barley yellow dwarf virus PAV coat protein gene stop codon. *J. Virol.*, **70**, 5884–92.
60. Steneberg,P. and Samakovlis,C. (2001) A novel stop codon readthrough mechanism produces functional Headcase protein in *Drosophila* trachea. *EMBO Rep.*, **2**, 593–597.
61. Schuller,A.P., Wu,C.C.-C., Dever,T.E., Buskirk,A.R. and Green,R. (2017) eIF5A Functions Globally in Translation Elongation and Termination. *Mol. Cell*, **66**, 194–205.e5.
62. Pelechano,V. and Alepuz,P. (2017) eIF5A facilitates translation termination globally and promotes the elongation of many non polyproline-specific tripeptide sequences. *Nucleic Acids Res.*, **45**, 7326–7338.
63. Brown,A., Shao,S., Murray,J., Hegde,R.S. and Ramakrishnan,V. Structural basis for stop codon recognition in eukaryotes. 10.1038/nature14896.
64. Matheisl,S., Berninghausen,O., Becker,T. and Beckmann,R. (2015) Structure of a human translation termination complex. *Nucleic Acids Res.*, **43**, 8615–8626.
65. Chung,B.Y.-W., Firth,A.E. and Atkins,J.F. (2010) Frameshifting in alphaviruses: a diversity of 3' stimulatory structures. *J. Mol. Biol.*, **397**, 448–56.
66. Iakoucheva,L.M., Kimzey,A.L., Masselon,C.D., Bruce,J.E., Garner,E.C., Brown,C.J., Dunker,A.K., Smith,R.D. and Ackerman,E.J. (2001) Identification of intrinsic order and disorder in the DNA repair protein XPA. *Protein Sci.*, **10**, 560–571.
67. Jones,P., Binns,D., Chang,H.-Y., Fraser,M., Li,W., McAnulla,C., McWilliam,H., Maslen,J., Mitchell,A., Nuka,G., *et al.* (2014) InterProScan 5: genome-scale protein function classification. *Bioinformatics*, **30**, 1236–40.
68. Marchler-Bauer,A., Derbyshire,M.K., Gonzales,N.R., Lu,S., Chitsaz,F., Geer,L.Y., Geer,R.C., He,J., Gwadz,M., Hurwitz,D.I., *et al.* (2015) CDD: NCBI's conserved domain database. *Nucleic Acids Res.*, **43**, D222-6.
69. Saijo,T., Ito,M., Takeda,E., Huq,A.H., Naito,E., Yokota,I., Sone,T., Pike,J.W. and Kuroda,Y. (1991) A unique mutation in the vitamin D receptor gene in three Japanese patients with vitamin D-dependent rickets type II: utility of single-strand conformation polymorphism analysis for heterozygous carrier detection. *Am. J. Hum. Genet.*, **49**, 668–73.
70. Arai,H., Miyamoto,K., Taketani,Y., Yamamoto,H., Iemori,Y., Morita,K., Tonai,T., Nishisho,T., Mori,S. and Takeda,E. (1997) A vitamin D receptor gene polymorphism in the translation initiation codon: effect on protein activity and relation to bone mineral density in Japanese women. *J. Bone Miner. Res.*, **12**, 915–21.
71. Jurutka,P.W., Remus,L.S., Whitfield,G.K., Thompson,P.D., Hsieh,J.C., Zitzer,H., Tavakkoli,P., Galligan,M.A., Dang,H.T., Haussler,C.A., *et al.* (2000) The polymorphic N terminus in human

Downloaded from http://www.jbc.org/ by guest on February 27, 2018

vitamin D receptor isoforms influences transcriptional activity by modulating interaction with transcription factor IIB. *Mol. Endocrinol.*, **14**, 401–20.
72. Crofts,L.A., Hancock,M.S., Morrison,N.A. and Eisman,J.A. (1998) Multiple promoters direct the tissue-specific expression of novel N-terminal variant human vitamin D receptor gene transcripts. *Proc. Natl. Acad. Sci. U. S. A.*, **95**, 10529–34.
73. Sunn,K.L., Cock,T.-A., Crofts,L.A., Eisman,J.A. and Gardiner,E.M. (2001) Novel N-Terminal Variant of Human VDR. *Mol. Endocrinol.*, **15**, 1599–1609.
74. Gardiner,E.M., Esteban,L.M., Fong,C., Allison,S.J., Flanagan,J.L., Kouzmenko,A.P. and Eisman,J.A. (2004) Vitamin D receptor B1 and exon 1d: functional and evolutionary analysis. *J. Steroid Biochem. Mol. Biol.*, **89–90**, 233–238.
75. Fixsen,S.M. and Howard,M.T. (2010) Processive selenocysteine incorporation during synthesis of eukaryotic selenoproteins. *J. Mol. Biol.*, **399**, 385–396.
76. Suzuki,K., Bose,P., Leong-Quong,R.Y.Y., Fujita,D.J. and Riabowol,K. (2010) REAP: A two minute cell fractionation method. *BMC Res. Notes*, **3**, 294.
77. Dmitriev,R.I., Zhdanov,A. V., Nolan,Y.M. and Papkovsky,D.B. (2013) Imaging of neurosphere oxygenation with phosphorescent probes. *Biomaterials*, **34**, 9307–9317.
78. Harrow,J., Frankish,A., Gonzalez,J.M., Tapanari,E., Diekhans,M., Kokocinski,F., Aken,B.L., Barrell,D., Zadissa,A., Searle,S., *et al.* (2012) GENCODE: The reference human genome annotation for The ENCODE Project. *Genome Res.*, **22**, 1760–1774.
79. Blanchette,M., Kent,W.J., Riemer,C., Elnitski,L., Smit,A.F.A., Roskin,K.M., Baertsch,R., Rosenbloom,K., Clawson,H., Green,E.D., *et al.* (2004) Aligning multiple genomic sequences with the threaded blockset aligner. *Genome Res.*, **14**, 708–15.
80. Kent,W.J., Sugnet,C.W., Furey,T.S., Roskin,K.M., Pringle,T.H., Zahler,A.M. and Haussler,D. (2002) The human genome browser at UCSC. *Genome Res.*, **12**, 996–1006.

FIGURE LEGENDS

Figure 1. Readthrough efficiencies determined by dual luciferase assay after transfection of HEK293T cells with dual luciferase reporter constructs consisting of candidate sequences (6 nt 5' and 12 nt 3' of stop codon (9 nt 3' for MS4A5 because of an in-frame stop codon)) shown in Supp. Table 1. *AQP4* readthrough has been described previously (17, 21) and is included here as an internal readthrough control. A UGA_C control indicated by a dashed line represents background readthrough levels. In each box-whisker plot center lines show the medians; box limits indicate the 25th and 75th percentiles as determined by R software; whiskers extend 1.5 times the interquartile range from the 25th and 75th percentiles, outliers are represented by dots. n = 12 biological replicates.

Figure 2. CodAlignView image of the placental-mammal alignment of the VDR readthrough region with 10-codon context on each side. A 1-base deletion in the human lineage in the 19th codon (indicated by highlighted Q) shifted the theoretical translation frame in Old and New World monkeys from that of Bushbaby and more distantly related species. A substitution in the second stop codon in Marmoset suggests that readthrough might not have been functional in Old World monkeys until after they split from New World monkeys. The open reading frame is conserved in all of the Old World monkeys except Gibbon, in which a 1-base deletion in the 45th codon shifts the reading frame.

Figure 3. A) Western blots of protein lysates and anti-HA immunoprecipitates prepared from HEK293T cells either mock-transfected (M) or transfected with HA-VDR-TGA (TGA), HA-VDR-TGG (TGG) or HA-VDR-TAATAA (TAA) as indicated. Anti-VDRx is a custom polyclonal antibody raised in rabbit against the full 67 amino acid VDR readthrough peptide. * indicates immunodetection of the IgG heavy chain. B) Western blots of cytoplasmic and nuclear fractions from HEK293T cells either mock-transfected (M) or transfected with HA-VDR-TAATAA (TAA) or HA-VDR-TGG (TGG) as indicated. EEF2 is eukaryotic elongation factor 2 located predominantly in the cytoplasm and DNMT3B is DNA methyltransferase 3 beta located predominantly in the nucleus. C) Western blots of protein lysates and

Downloaded from http://www.jbc.org/ by guest on February 27, 2018

anti-GFP immunoprecipitates prepared from HEK293T cells co-transfected with the indicated expression constructs. HA-eRF1 is a HA-tagged eukaryotic release factor 1 used here as a negative control.

Figure 4. (A) Relative luciferase activities determined by dual luciferase assay after co-transfection of HEK293T cells with plasmids expressing HA-tagged VDR proteins (or mock transfected) as indicated, together with firefly luciferase reporter constructs driven by a minimal promoter with either tandem VDR elements (VDRE) from the rat osteocalcin gene (WT) or control firefly luciferase reporters harboring mutated VDREs (Mu). A *Renilla* luciferase plasmid was also co-transfected to allow firefly luciferase activity normalization. Transfectants that were treated with vehicle (ethanol) control are indicated by the minus symbol and the plus symbol indicates activities from calcitriol-stimulated (1 nM) cells. Representative anti-HA western blot of the same lysates are shown under the histogram. In each box-whisker plot center lines show the medians; box limits indicate the 25th and 75th percentiles as determined by R software; whiskers extend 1.5 times the interquartile range from the 25th and 75th percentiles, outliers are represented by dots. n = 4 biological replicates. (B) Relative luciferase activities determined by dual luciferase assay of HEK293T cells transfected as in (A) then treated with varying concentrations of calcitriol as indicated for 24 hr. Dashed lines indicate relative luciferase activities when HA-RXRα was co-transfected along with VDR variants. Means and standard deviations are shown from n=8 biological replicates.

Downloaded from http://www.jbc.org/ by guest on February 27, 2018

Figure 1

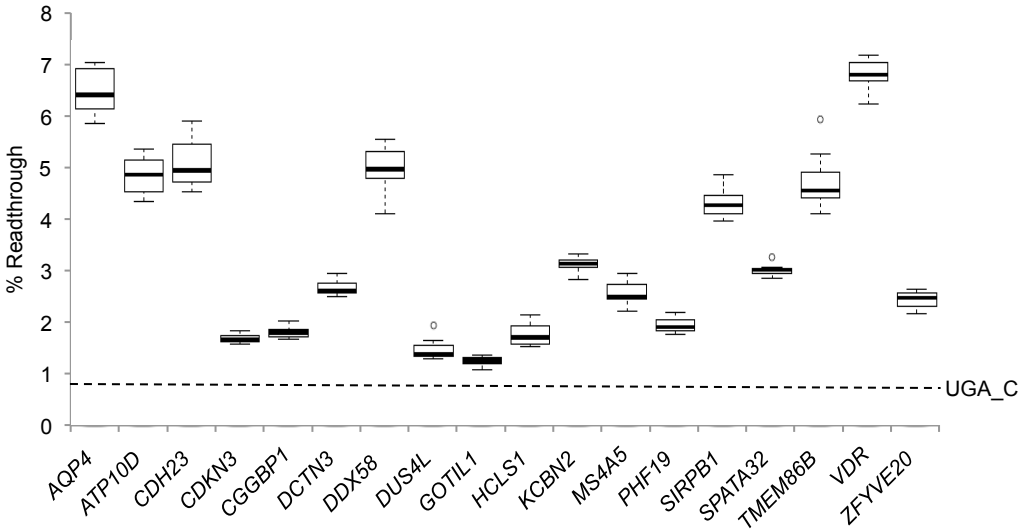
% Readthrough
8
7
6
5
4
3
2
1
0
UGA_C
AQP4
ATP10D
CDH23
CDKN3
CGGBP1
DCTN3
DDX58
DUS4L
GOTIL1
HCLS1
KCBN2
MS4A5
PHF19
SIRPB1
SPATA32
TMEM86B
VDR
ZFYVE20

Figure 2

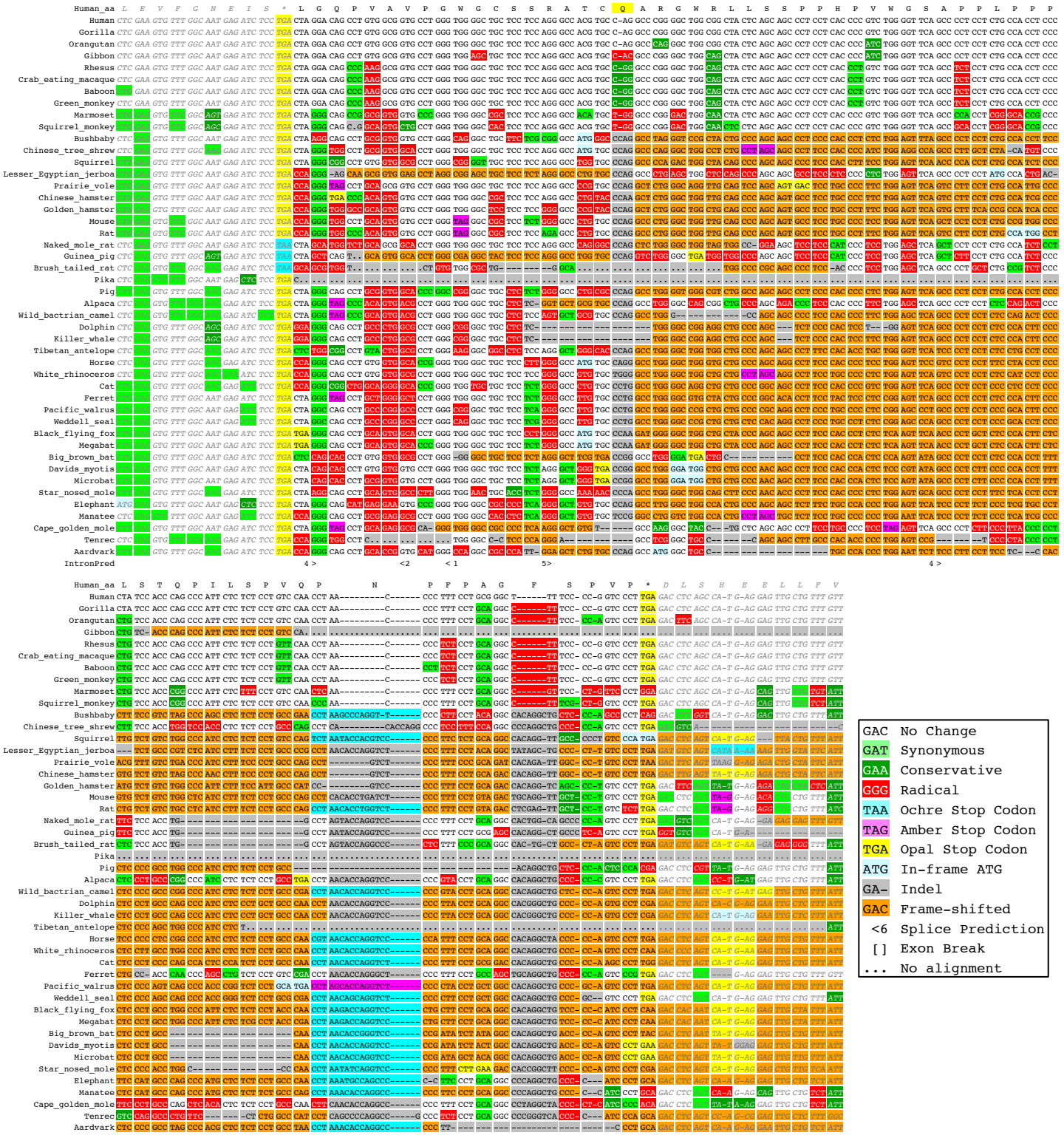
GAC No Change
GAT Synonymous
GAA Conservative
GGG Radical
TAA Ochre Stop Codon
TAG Amber Stop Codon
TGA Opal Stop Codon
ATG In-frame ATG
GA- Indel
GAC Frame-shifted
<6 Splice Prediction
[] Exon Break
... No alignment

Figure 3

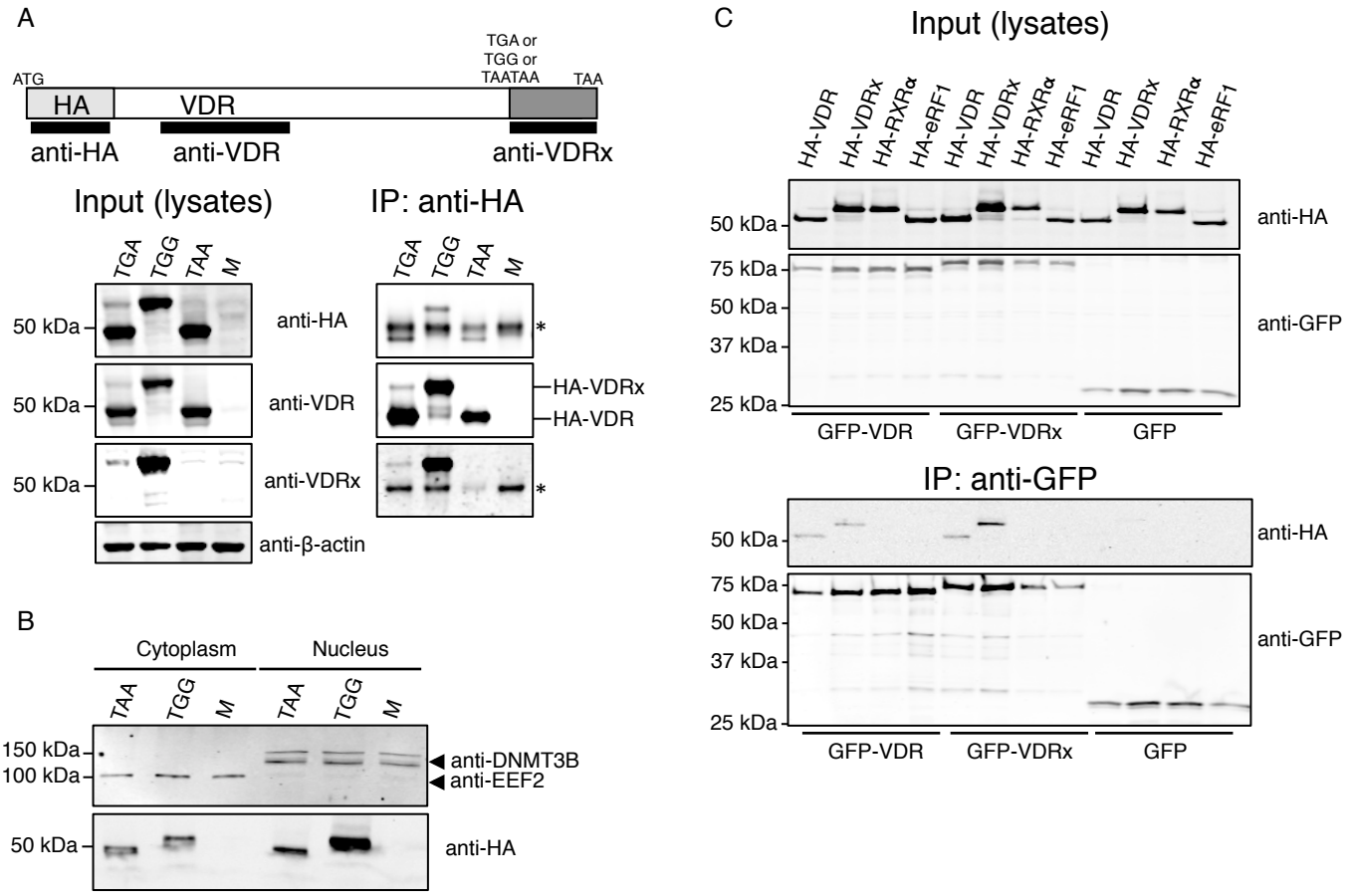
A
ATG
HA
VDR
TGA or
TGG or
TAATAA
TAA
anti-HA
anti-VDR
anti-VDRx
Input (lysates)
IP: anti-HA
TGA
TGG
TAA
M
50 kDa
anti-HA
anti-VDR
anti-VDRx
anti-β-actin
HA-VDRx
HA-VDR
B
Cytoplasm
Nucleus
150 kDa
100 kDa
anti-DNMT3B
anti-EEF2
anti-HA
C
Input (lysates)
HA-VDR
HA-VDRx
HA-RXRα
HA-eRF1
75 kDa
37 kDa
25 kDa
anti-GFP
GFP-VDR
GFP-VDRx
GFP
IP: anti-GFP

Figure 4

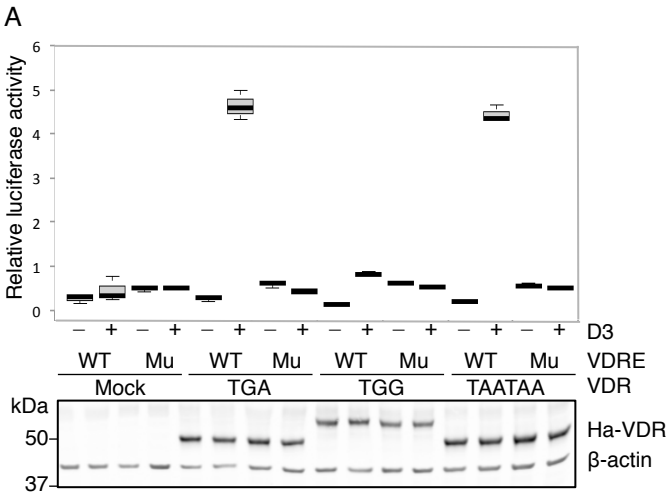
A
Relative luciferase activity
6
5
4
3
2
1
0
– + – + – + – + – + – + – + – + D3
WT Mu WT Mu WT Mu WT Mu VDRE
Mock TGA TGG TAATAA VDR
kDa
50
37
Ha-VDR
β-actin

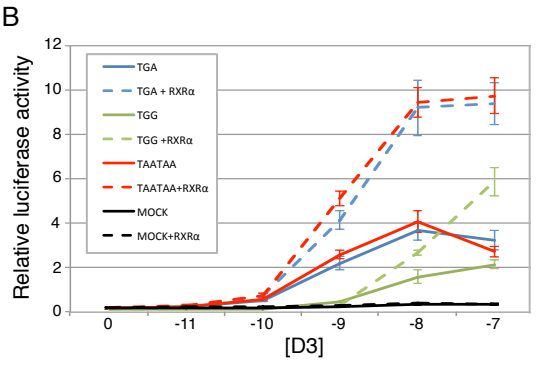
B
Relative luciferase activity
12
10
8
6
4
2
0
TGA
TGA + RXRα
TGG
TGG +RXRα
TAATAA
TAATAA+RXRα
MOCK
MOCK+RXRα
0 -11 -10 -9 -8 -7
[D3]

Stop codon readthrough generates a C-terminally extended variant of the human vitamin D receptor with reduced calcitriol response

Gary Loughran, Irwin Jungreis, Ioanna Tzani, Michael Power, Ruslan I Dmitriev, Ivaylo P Ivanov, Manolis Kellis and John F Atkins

J. Biol. Chem. published online January 31, 2018

Access the most updated version of this article at doi: 10.1074/jbc.M117.818526

Alerts:
- When this article is cited
- When a correction for this article is posted

Click here to choose from all of JBC's e-mail alerts

Downloaded from http://www.jbc.org/ by guest on February 27, 2018